Research Article | Vol. 32, No. 11 / 20 May 2024 / Optics Express 19221
Optics EXPRESS

Noninvasive characterization methods for ultra-short laser pulse induced volume modifications

MAX STEUDEL,[1,*] MAX-JONATHAN KLEEFOOT,[1] SEBASTIAN FUNKEN,[1] ALEXANDER BANHOLZER,[2] MARIO WOLF,[3] SILVIA SCHUHMACHER,[4] UWE MORGNER,[5] AND ANNE HARTH[1]

[1]*Center of Optical Technologies, Aalen University, Aalen, Germany*
[2]*Carl Zeiss Microscopy GmbH, Oberkochen, Germany*
[3]*PVA TePla Analytical Systems GmbH, Westhausen, Germany*
[4]*Department of Applied Surface and Material Sciences, Aalen University, Aalen, Germany*
[5]*Institute of Quantum Optics, Leibniz University Hannover, Hannover, Germany*
[*]*max.steudel@hs-aalen.de*

Abstract: We present two noninvasive characterization methods to investigate laser induced modifications in bulk fused silica glasses. The methods discussed are immersion microscopy and scanning acoustic microscopy (SAM). SAM shows merits in measuring the distance from sample surface to the first detectable density change of the modification, while immersion microscopy offers a look into the modification. Both noninvasive methods are preferred over conventional polishing or etching techniques due to the facts, that multiple investigations can be done with only one sample and lower time expenditure. The type II modifications were introduced by focusing laser pulses with high repetition rates into the fused silica.

1. Introduction

The characterization of light-matter interaction is the backbone of optic experiments, which led to numerous applications but also new questions regarding the control of light [1–3]. In the case of volume modification induced by ultra-short laser pulses (uslp) into glasses, characterization is typically done afterwards [4–6], but e.g. in-situ pump-probe experiments [3] paved the way for understanding the process. To gain knowledge about internal structures, currently the state of the art is to perform cross section cutting [7–9] and/or chemical etching [6,10,11]. Typically, the samples are then investigated by optical microscopy [8], with atomic force microscopy [10], Raman spectroscopy [7,11] or transmission electron microscopy [9]. Chemical etching generally involves highly corrosive hydrofluoric acid, which is needed because of the chemical stability of glasses. Cutting the sample has the disadvantage, besides the long polishing times afterwards, that the sample is mechanically disrupted, leading to tension within the sample. Furthermore, cutting the sample in half will affect the tensile test, since the sample's structure is changed in the cut area.

Since these techniques show major disadvantages i.e., they are either time consuming, employ dangerous chemicals and physically manipulate the sample, we investigated a different direction: the noninvasive characterization of uslp induced volume modifications. A method, which is already used in research and industry for this purpose is the optical coherence tomography [12]. We don't address this technique further.

In this paper we want to show two more alternative and noninvasive investigation methods which are scanning acoustic microscopy (SAM) and immersion microscopy. Both techniques circumvent the requirement for polishing/grinding and etching, which are all immensely time intensive and mechanically disrupt the sample. Immersion microscopy is an optical characterization technique

#515308 https://doi.org/10.1364/OE.515308
Journal © 2024 Received 6 Dec 2023; revised 16 Feb 2024; accepted 11 Mar 2024; published 10 May 2024

Optics EXPRESS

with the benefit that it is available in most of the laboratories, it reduces time effort, the technique does not apply any stress into the material, and thus allows for further non-invasive investigations. The paper is organized as follows: firstly we introduce the laser system we used to produce the volume modifications which were studied via immersion microscopy (section 3) and with SAM (section 4). We end with a conclusion.

2. Laser characteristics

In this work the volume modifications in fused silica glasses were produced by a commercial 20 W uslp laser (TRUMPF TruMicro 2020) which delivers linear polarized pulses with a pulse duration of about 350 fs. The central wavelength of this laser is 1030 nm, repetition rate was set to 1 MHz and pulse energy was varied. The complete system shown in Fig. 1, visualizes the beam path from the laser to the fused silica samples. To ensure that the electric field of the laser pulse at the interaction zone has no preferred polarization direction, a quarter wave plate was installed to ensure circular polarization.

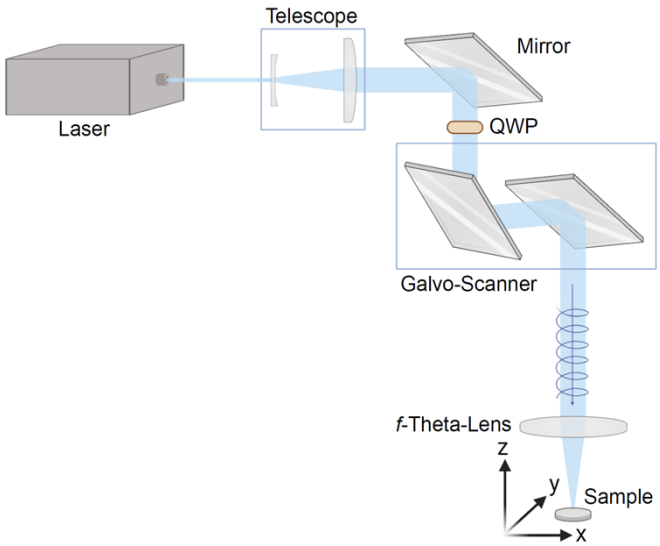

Fig. 1. Schematic laser setup with a quarter wave plate (QWP), leading to a circular polarized beam indicated by the blue helical line. The Galvo-Scanner controls the deflection of the beam.

By using a telescope to enlarge the raw-beam and a f-theta-lens with a focal length of 100 mm, a focal diameter of 16 µm ($1/e^2$) was achieved. Fused silica cylinders with 1 inch diameter and 3 mm height were processed. The critical power $P_{crit} = \pi(0.61)^2\lambda_0^2/(8n_0n_2)$ [13] for fused silica of 4.4 MW was exceeded even for the lowest used energy of 12.7 µJ by far (~36 MW). Thus, this work examines modifications resulting from the filamentation regime, like Kahle et. al [14] and Gstalter et. al. [15]. The top sides of the sample were polished and cleaned beforehand to minimize aberrations in the laser process, while the lateral surface remained unpolished.

3. Immersion microscopy

The method of using an immersion oil in order to increase resolving power of an optical system is widely used [16,17]. In our case, immersion microscopy is performed differently to the general understanding of the method, where immersion is used to increase the microscope numerical aperture. Here, the immersion oil is employed to reduce scattering at the unpolished side of the

Optics EXPRESS

sample. Therefore, the whole sample has to be surrounded by the immersion oil. A schematic illustration can be found in Fig. 2.

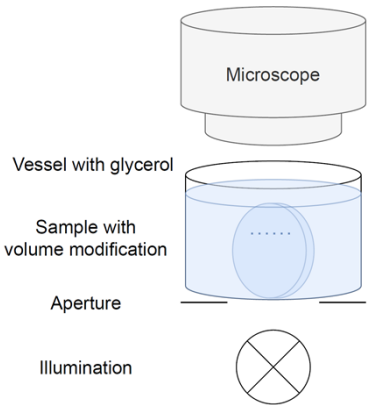

Fig. 2. Immersion microscopy scheme. The sample is placed vertically into the glycerol, so that the cross section of the volume modifications becomes visible.

Glycerol is applied as refractive index matching oil. The refractive indices of glycerol (1.4739, [18]) and fused silica (1.4585, [19]) match quite good ($\Delta n \approx 0.015$). Due to the small difference, it is still possible to detect the samples surface, if the sample is placed exactly perpendicular in the vessel. A microscope with long working distances allows the analysis of a large sample. The microscope used in this work was the ZEISS Axiozoom V-16 with the PlanNeoFluar Z 2.3x objective. Compared to other microscopes it already achieves a high aperture in the medium zoom range, which is a compelling attribute for our investigation. This microscope also allows for three different illumination settings: brightfield, darkfield and oblique transmitted light.

For the immersion microscopy a sample with varying laser parameters was produced. Closely spaced volume modifications would cause optical distortions, resulting in a poor image. Thus, the distance between the modifications was set to 0.5 mm. To visualize the induced modifications a polariscope image, taken with the polariscope StrainScope from the company ilis GmbH. of the sample can be seen in Fig. 3(a).

The measured retardation of the light corresponds to changes in the refractive index and induced stresses. To demonstrate repeatability, the same patterns were inscribed three times for each parameter set. On the left- and right-hand side, the number of pulses per point was kept fixed (left: 1000 pulses, right: 100 pulses) and the energy was linearly changed from 13.1 µJ to 16.4 µJ, while on top and bottom the energy was kept fixed (top: 16.4 µJ, bottom: 14.8 µJ) and the pulses per point where changed from 1 to 1000 pulses per point (according to the top label in Fig. 4). Since the number of pulses per point were changed by three orders of magnitude, the modifications with high number of pulses per point show a more prominent signal in retardation, corresponding to a large change in density and/or induced stresses. Figure 3(b) shows the unpolished lateral surface which becomes opaque when placing the sample into the immersion setup, like shown in Fig. 2.

The immersion microscope results of the modifications at the middle of the bottom part, where the energy was kept fixed at 16.4 µJ, are shown in Fig. 4, since they are reprensentative.

Immersion microscopy offers a look into modifications and enables width and length measurement of each modification. The microscope images were taken in the brightfield illumination setting and in order to save space, we only show results of the brightfield illumination setting, other settings were also capable of showing the modifications. In the images the inner teardrop structure becomes visible and voids, resulting from a vaporization process, appear. Since the glycerin is not perfectly index matched to the fused silica, the sample border remains visible. If

Optics EXPRESS

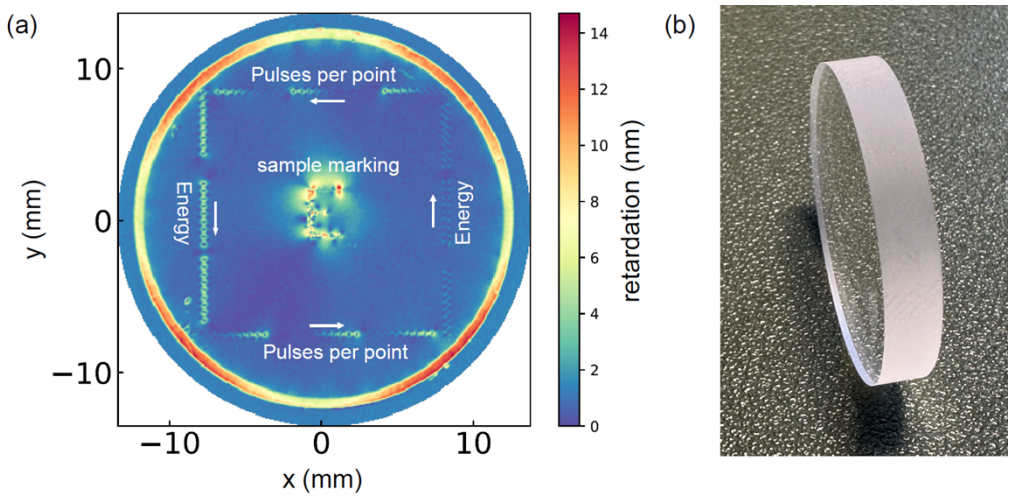

Fig. 3. (a) Polariscope image of the sample used for immersion microscopy. Pulses per point were kept fixed for modifications on the left and right at 1000 and 100 pulses per point. Energy was kept fixed at top and bottom at 16.4 µJ and 14.8 µJ, respectively. (b) Side view of the unpolished lateral surface of the sample

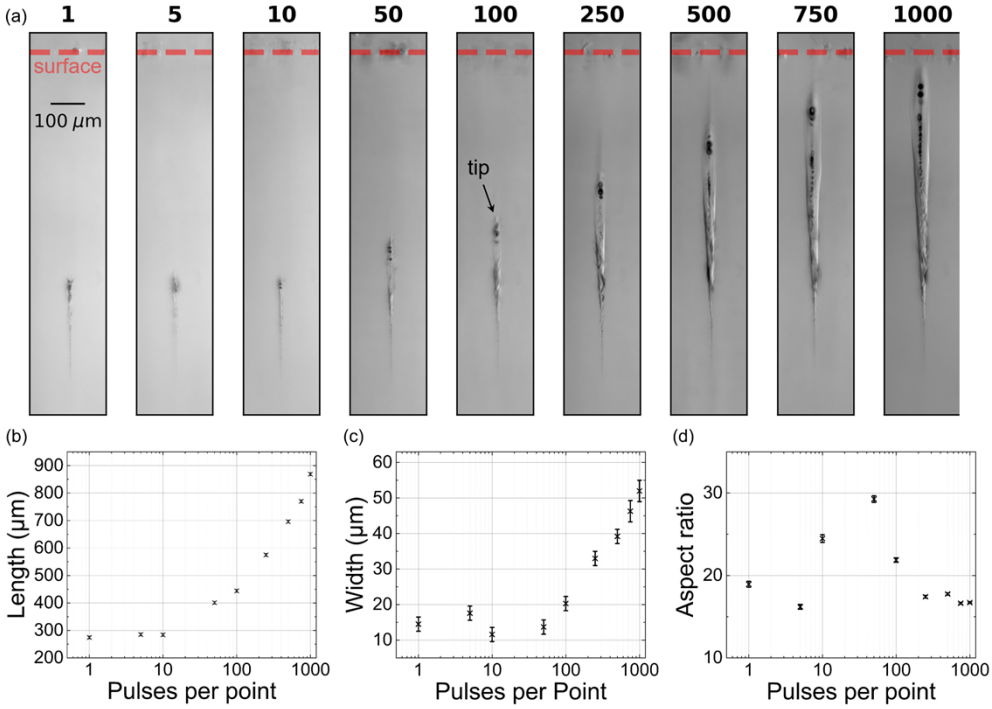

Fig. 4. Immersion microscopy images of the laser induced volume modifications at different number of pulses per point and constant pulse energy (a). The dashed red line indicates the surface of the sample. Length (b), width (c) and aspect ratio (d) dependence on pulses per point are shown.

Optics EXPRESS

the sample is exactly aligned to the microscope axis, it would be possible to estimate the distance from the tip of the modification relative to the sample border. With increasing number of pulses per point the overall size of the modification increases and as a consequence also the postion of the modifications tip moves closer to the surface, since the focal z-postion was kept the same for all laser modifications. Figure 4 shows not a linear behaviour in length (b) when using more than 10 pulses per point. The width is defined as maximum width of the modification and it also changes when more than 10 pulses per point are used. Interestingly, the aspect ratio remains nearly the same for small and large numbers of pulses. The measurement inaccuracy indicated as error bars in Fig. 4 is due to the reading error in the pixel area of the microscopic picture. The uncertainty of the width and length measurement is estimated as ± 3 and ± 5 microns, respectively.

As shown in different publications, the teardrop shape emerges also at stronger focussing conditions [4,20,21] and can even be simulated [22,23,6]. A stonger focus leads to a more bellied modification with lower aspect ratio than the modifications shown here. Since the laser parameters are comparable, only the focussing technique can be responsible for this effect. As the energy is deposited over a wider range than in the strong focussing regime, no elliptic heat affected zone is visible for our modifications.

Since we used a light microscope, we will have a lower resolution than e.g. with transmission electron microscopy (TEM) [9], but the effort involved must be set in relation to the yield. If the TEM resolution is not needed and the resolution of the light microscope is sufficient, the immersion microscopy method described, can save a lot of effort and time.

4. Scanning acoustic microscopy

Scanning acoustic measurements were carried out with a commercial setup from PVA TePla called SAM301. The sample was placed in water to adjust the acoustic impedance and thus couple more acoustic energy into the sample. A focusing transducer (Fig. 5(a)) emits a pulse of ultrasonic waves and receives the reflected and backscattered waves from the sample after a certain time delay (Fig. 5(b)). The transducer consists of a piezoelectric oscillator and an acoustic lens with a focal length of 5.9 mm in water.

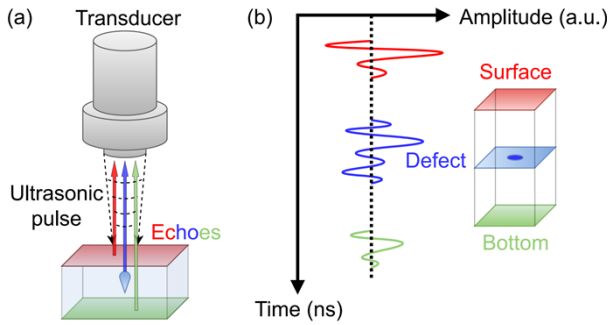

Fig. 5. Scheme of the incident and reflected ultrasonic pulse (a) and time-dependent changes of the echoes amplitude (b) (analog to [25]).

By vertically changing the position of the transducer relative to the sample, the focusing position is adjusted. With a center frequency of 125 MHz of the ultrasonic pulse, the spot size results at about 30 µm in the focal plane. As the resolution decreases dramatically out of the focus, the Synthetic Aperture Focusing Technique (SAFT) is applied to obtain highly resolved images in all depths [24]. SAFT is a reconstruction method that employs the information from multiple pulse-echo measurements. By superimposing signals from various scan positions, a virtual, larger aperture is created, enabling a full volume reconstruction and the detection of

Optics EXPRESS

structures in various depths. A comprehensive review of this method can be found e.g. in these publications [25,24,26–28].

The scanning acoustic microscope experiments were performed on another fused silica sample processed with varying laser parameters. The focal position inside the glass was kept the same for all laser parameters. A field of volume modifications, where the pulse energy was changed from 12.7 µJ to 16.4 µJ in x-direction and the number of pulses per point was changed from 1 to 2000 in y-direction (Fig. 6), was created.

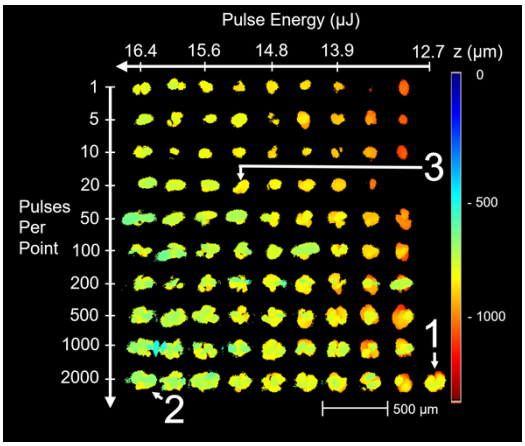

Fig. 6. Time of flight (TOF) data of the volume modifications tip relative to the surface of the sample (z = 0). The laser parameters pulse energy and pulses per point were changed according to the arrows surrounding the field. The numbers 1-3 indicate the positions of the A-scans depicted in Fig. 7.

The focus in Fig. 6 was set in the upper right corner of the modification field. This leads to an incorrect visualization of the other modification shapes - especially at the lower left side - since these modifications are out of focus. Note, that these modifications are out of focus, because a higher number of pulses per point corresponds to a growth of the modification towards the surface (see section 3). As the TOF data is only slightly dependent on the focusing position, it can be assumed that the z-heights shown, nevertheless correspond to changes in density and sound velocity.

As expected, the scan shows large distances from the surface to the modification tip for low energy and only few pulses per point. Because the laser focal position was kept fixed for all modifications, a large distance from surface to modification (indicated red in Fig. 6) corresponds to a less pronounced modification with a small melt volume.

On the other hand, modifications with higher pulse energy and more pulses per point appear closer to the surface, indicating a bigger melt volume. To qualify the distance from surface to the tip of the modification, three points, indicated by numbers 1-3 in Fig. 6, were chosen exemplarily. Figure 7(a) shows the A-scans of these measurement points. The A-scan provides local time-of-flight (TOF) information along the z-axis from the ultrasonic wave.

The time axis in Fig. 7(a) does not start at zero since the ultrasound pulse needs time to travel from the transducer to the sample. When the first surface signal is detected, the acquisition of data will start. Since we mainly focus on investigating the volume modifications signal, the surface signal gets overamplified. The differences from the modification signals of point 1 and 2 are difficult to recognize in Fig. 7(a). To increase the visibility of the signal change, an autocorrelation for the modification signal of the A-scan from point 1 was calculated. Additionally, cross-correlations for the modification signals from point 2 and 3 with the modification signal

Optics EXPRESS

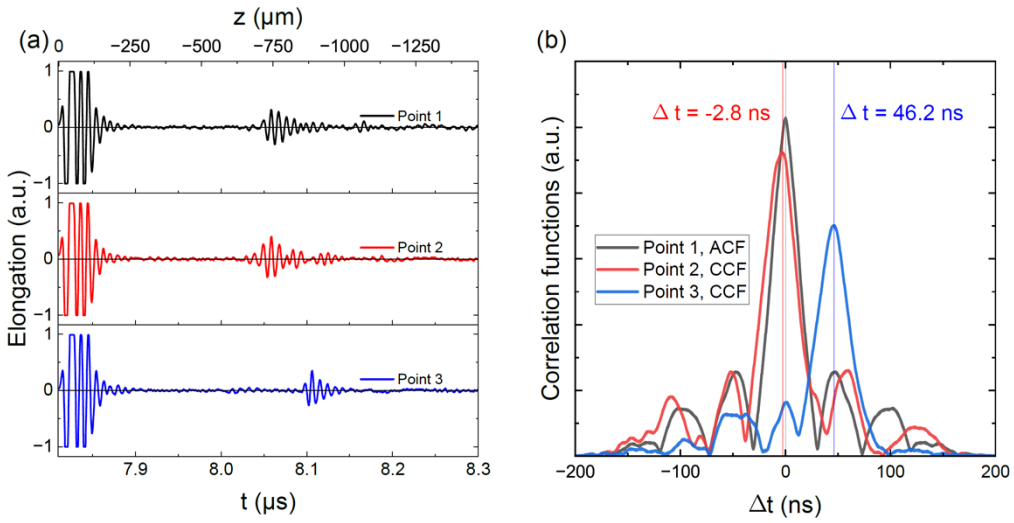

Fig. 7. (a) A-scans of the points 1-3 indicated in Fig. 6. The elongation refers to the displacement of the piezoelectric element in the transducer, which is then electrically digitalized and amplified. (b) Autocorrelation function of the modifications signal from point 1 and cross-correlation functions of the modifications signal from point 2 and 3 with the modification signal of point 1.

from point 1 were carried out. The maxima of the correlation function from point 2 and 3 are shifted with respect to the autocorrelation of point 1. This indicated relative time delay Δt corresponds to a z-shift of the modification.

The relative position z is calculated by multiplying the sound velocity of fused silica (6 km/s, [29]) with the time delay Δt and divide by a factor of two, since the wave needs to travel the path twice. This results in a change of – (8.4 ± 1.0) µm for point 2 and (138.6 ± 1.0) µm for point 3 for the z-position relative to point 1, like shown in Table 1.

Table 1. Pulse energy E_p, pulses per point # used for the modifications 1, 2 and 3 resulting in different time delays Δt and relative z-positions to modification 1.

Modification	E_p (µJ)	#	Δt (ns)	z (µm)
1	12.7	2000	0	0
2	16.4	2000	- 2.8	– 8.4 ± 1.0
3	15.2	20	46.2	138.6 ± 1.0

The measurement error results from uncertainties in position of the peak and in uncertainties of the sound velocity, since fused silica is an amorphous material. The calculated height differences correspond to the used laser parameters, since bigger melt volumes are expected at higher pulse energy and more pulses per point.

5. Conclusion

This paper showed a comparison of two noninvasive imaging techniques for the visualization of laser-induced bulk modifications in fused silica. Avoiding the cutting and polishing steps allows for a qualitative analysis of the samples directly after processing with the advantage to continue characterization of the same sample, while maintaining its physical properties.

With SAM the first interface of the modifications becomes visible. This could be used to measure and calculate the depth from surface to upper part of the modifications. Smaller voids

Optics EXPRESS

and bubbles could not be identified with this method. Further focusing of the ultrasonic pulses could help to investigate these voids, which will be a part of further investigations. The big challenge there is to still have a large penetration depth while improving the resolution.

SAM determines the z-position of the modification tip relative to the surface accurate via TOF-measurements. This particular distance is difficult to measure with immersion microscopy, since even a small tilt of the sample will lead to reflections of the illumination and therefore distort the image. However, immersion microscopy reveals the complete 2D structure of the laser induced modification. Since resolution of this technique comes with a tradeoff in working distance, it becomes handy to use stereomicroscopes.

Based on the results shown, it was demonstrated that both methods can be used for the noninvasive investigations of volume modifications in fused silica. The advantages of immersion microscopy are the simple and rapid examination using a stereomicroscope and glycerol. The use of SAM, on the other hand, is more time-consuming and requires more expertise regarding the handling of the system and post-processing but allows for a more precise measurement of the distance from surface to the tip of the modification. As an outlook SAM shows some potential for analyzing laser-modified optical materials which are not restricted to glass, including polymers [30,31] and semiconductors [32].

Funding. Deutsche Forschungsgemeinschaft (512645013); Bundesministerium für Bildung und Forschung (13FH 135KX0).

Acknowledgments. We acknowledge Hochschule Aalen (Aalen, Germany), the Carl Zeiss Microscopy GmbH and members of the PVA TePla GmbH for support and/or provision of experimental facilities.

Disclosures. We disclose no conflict of interests.

Data availability. Data and materials used in the analysis are available in the text, methods or from the authors upon reasonable request.

References

1. Y. Schrödel, C. Hartmann, J. Zheng, *et al.*, "Acousto-optic modulation of gigawatt-scale laser pulses in ambient air," Nat. Photon. **18**(1), 54–59 (2024).
2. R. R. Gattass and E. Mazur, "Femtosecond laser micromachining in transparent materials," Nat. Photonics **2**(4), 219–225 (2008).
3. K. Bergner, B. Seyfarth, K. A. Lammers, *et al.*, "Spatio-temporal analysis of glass volume processing using ultrashort laser pulses," Appl. Opt. **57**(16), 4618–4632 (2018).
4. S. M. Eaton, H. Zhang, P. R. Herman, *et al.*, "Heat accumulation effects in femtosecond laser-written waveguides with variable repetition rate," Opt. Express **13**(12), 4708–4716 (2005).
5. S. R. McArthur, R. R. Thomson, and C. A. Ross, "Investigating focus elongation using a spatial light modulator for high-throughput ultrafast-laser-induced selective etching in fused silica," Opt. Express **30**(11), 18903–18918 (2022).
6. I. Miyamoto, Y. Okamoto, R. Tanabe, *et al.*, "Mechanism of dynamic plasma motion in internal modification of glass by fs-laser pulses at high pulse repetition rate," Opt. Express **24**(22), 25718–25731 (2016).
7. S. Richter, F. Zimmermann, A. Tünnermann, *et al.*, "Laser welding of glasses at high repetition rates-Fundamentals and prospects," Opt. Laser Technol. **83**, 59–66 (2016).
8. F. Zimmermann, S. Richter, S. Döring, *et al.*, "Ultrastable bonding of glass with femtosecond laser bursts," Appl. Opt. **52**(6), 1149–1154 (2013).
9. T. Gorelik, M. Will, S. Nolte, *et al.*, "Transmission electron microscopy studies of femtosecond laser induced modifications in quartz," Appl. Phys. A **76**(3), 309–311 (2003).
10. V. R. Bhardwaj, E. Simova, P. P. Rajeev, *et al.*, "Optically produced arrays of planar nanostructures inside fused silica," Phys. Rev. Lett. **96**, 57404 (2006).
11. D. J. Little, M. Ams, P. Dekker, *et al.*, "Femtosecond laser modification of fused silica: the effect of writing polarization on Si-O ring structure," Opt. Express **16**(24), 20029–20037 (2008).
12. S. Hecker, R. Weber, and T. Graf, "Position sensing of ultrashort pulsed laser-welded seams in glass by optical coherence tomography," J. Laser Appl. **32**, 2 (2020).
13. R. W. Boyd, *Nonlinear Optics* (Elsevier: London, U.K., 2020).
14. M. Kahle and D. Nodop, "Glass welding with ultra-short laser pulses and long focal lengths A process model," Procedia CIRP **111**, 617–620 (2022).
15. M. Gstalter, G. Chabrol, A. Bahouka, *et al.*, "Long focal length high repetition rate femtosecond laser glass welding," Appl. Opt. **58**(32), 8858–8864 (2019).
16. S. M. Mansfield and G. S. Kino, "Solid immersion microscope," Appl. Phys. Lett. **57**(24), 2615–2616 (1990).

Optics EXPRESS

17. S. Owa and H. Nagasaka, "Immersion lithography; its potential performance and issues," in *Optical Microlithography XVI, SPIE Proceedings* (SPIE, 2003), p. 724.
18. V. Gupta, O. Aftenieva, P. T. Probst, *et al.*, "Advanced colloidal sensors enabled by an out-of-plane lattice resonance," Advanced Photonics Research **3**(11), 2200152 (2022).
19. I. H. Malitson, "Interspecimen comparison of the refractive index of fused silica*,†," J. Opt. Soc. Am. **55**(10), 1205 (1965).
20. S. Richter, F. Zimmermann, R. Eberhardt, *et al.*, "Toward laser welding of glasses without optical contacting," Appl. Phys. A **121**(1), 1–9 (2015).
21. S. Hecker, M. Blothe, and T. Graf, "Reproducible process regimes during glass welding by bursts of subpicosecond laser pulses," Appl. Opt. **59**(36), 11382–11388 (2020).
22. I. Miyamoto, K. Cvecek, and M. Schmidt, "Evaluation of nonlinear absorptivity in internal modification of bulk glass by ultrashort laser pulses," Opt. Express **19**(11), 10714–10727 (2011).
23. C. Kalupka, *Energiedeposition von ultrakurz gepulster Laserstrahlung in Gläsern; 1. Auflage, Dissertation*, RWTH Aachen University, 2019.
24. M. Wolf, P. Hoffrogge, E. Kuhnicke, *et al.*, "Inspection of multilayered electronic devices via scanning acoustic microscopy using synthetic aperture focusing technique," in *2022 IEEE International Ultrasonics Symposium (IUS)* (IEEE, 2022), pp. 1–4.
25. H. Yu, "Scanning acoustic microscopy for material evaluation," Applied Microscopy **50**, 1–11 (2020).
26. N. Hozumi, R. Yamashita, C.-K. Lee, *et al.*, "Time-frequency analysis for pulse driven ultrasonic microscopy for biological tissue characterization," Ultrasonics **42**(1-9), 717–722 (2004).
27. Z. Yu and S. Boseck, "Scanning acoustic microscopy and its applications to material characterization," Rev. Mod. Phys. **67**(4), 863–891 (1995).
28. R. A. Lemons and C. F. Quate, "Acoustic microscope—scanning version," Appl. Phys. Lett. **24**(4), 163–165 (1974).
29. E. M. Dianov, V. E. Fortov, I. A. Bufetov, *et al.*, "Detonation-like mode of the destruction of optical fibers under intense laser radiation," Jetp Lett. **83**(2), 75–78 (2006).
30. D. Perevoznik, A. Tajalli, D. Zuber, *et al.*, "Writing 3D waveguides with femtosecond pulses in polymers," J. Lightwave Technol. **39**(13), 4390–4394 (2021).
31. G.-L. Roth, C. Esen, and R. Hellmann, "Circular microchannels inside bulk polymethylmethacrylate generated by femtosecond laser using slit beam shaping," J. Laser Appl. **31**(2), 022603 (2019).
32. M. Chambonneau, D. Grojo, O. Tokel, *et al.*, "In-Volume Laser Direct Writing of Silicon—Challenges and Opportunities," Laser Photonics Rev. **15**(11), 2100140 (2021).